COMBINATION OF MR SURFACE COIL IMAGES USING WEIGHTED CONSTRAINED LEAST SQUARES

S. Derin Babacan[1]*, Xiaoming Yin*[1,2]*, Andrew C. Larson*[2]*, Aggelos K. Katsaggelos*[1]

[1]EECS Department
Northwestern University, Evanston, IL 60208, USA
sdb@northwestern.edu, xiaoming-yin@northwestern.edu, aggk@eecs.northwestern.edu

[2]Radiology
Northwestern University, Chicago, IL 60611
a-larson@northwestern.edu

ABSTRACT

For most MR imaging applications multiple surface coils are used to obtain images with high signal-to-noise ratios (SNR). However, signal intensity strongly diminishes with distance. Although there are a number of approaches to combine the surface coil images to obtain a high SNR and bias-free image, most of them are developed in an ad hoc manner and lack a systematic treatment. In this work we propose a new approach, an iterative weighted constrained least squares (WCLS) restoration method, for combining surface coil images. The algorithm is fully automated and outperforms approaches which appeared in the literature.

Index Terms— Magnetic resonance imaging, Least squares methods, parameter estimation, Image restoration

1. INTRODUCTION

Magnetic resonance imaging (MRI) has found many applications in the medical domain. The MRI scanner typically creates a magnetic field that alters the magnetization of the hydrogen atoms in the body and causes them to emit radio signals that are used to form the image of the desired tissue.

Images acquired by whole body coils are used in MRI which have homogeneous intensity distribution across the image (bias-free) but have low signal-to-noise ratios (SNRs). Recently it has been proposed to use an array of surface coils to obtain images with high SNRs [1, 2]. This approach, called "Nuclear Magnetic Resonance (NMR) phased array", is widely adapted in current MRI technology, and is based on simultaneously acquiring multiple images with closely positioned NMR receiver coils and combining these images after the acquisition. Although the surface coil images clearly have higher SNRs than whole body coil images, they are degraded by bias fields due to the locations of each surface coil since the intensity levels rapidly decrease with distance. In many applications it is desired to combine the surface coil images to obtain a high SNR and bias-free image.

The most common approach to combine the acquired images is the sum of squares (SOS) approach, where each pixel in the final image is the summation of the pixel in the coil images weighted by the coil sensitivities (bias fields). Although this approach provides a simple and fast solution to the problem, it can only result in lower SNR images and the bias is not completely removed. Alternative methods, both simple and complex, resulting in images with superior SNR have recently been proposed [3]. However, these approaches lack a systematic treatment of the unknown variables and the observations, and they are proposed in an ad hoc manner. There are other methods based on Bayesian blind deconvolution principles [4], but to our knowledge no work has been reported for combining the surface coil images when the bias fields are assumed to be known.

In this paper we provide a weighted constrained least squares formulation of the problem, and propose an iterative solution for combining the surface coil images. We also provide means to estimate the parameters in our model so that the proposed algorithm becomes fully automated. The experimental results demonstrate that the proposed algorithm clearly outperforms existing approaches with a low level of computational complexity.

This paper is organized as follows. In Sec. 2 we formulate the problem of combining the surface coil images as a constrained least squares problem. The iterative algorithm is presented in Sec. 3 and the choice of the weighting matrices for spatial adaptivity is discussed in Sec. 4. Experimental results are presented in Sec. 5 and conclusions are drawn in Sec. 6.

2. PROBLEM FORMULATION

Let the total number of surface coils be equal to m. The NMR phased array can be described mathematically as follows

$$\mathbf{g}_i = \mathbf{b}_i \otimes \mathbf{f} + \mathbf{n}_i, i = 1, ..., m, \quad (1)$$

where $\mathbf{g}_i$ denotes the i^{th} surface coil image, $\mathbf{f}$ is the unknown image of interest, and $\mathbf{b}_i$ and $\mathbf{n}_i$ denote the bias field (sensitivity) and the noise introduced by the i^{th} surface coil, respectively. We assume that all images are of size $p \times q$ and

that the noise $\mathbf{n}_i$ in each channel is additive Gaussian, but its variance can vary across channels. The operator $\otimes$ is the Kronecker product. The product of images $\mathbf{b}_i \otimes \mathbf{f}$ can be written as a matrix product by forming the $pq \times pq$ diagonal matrix $\mathbf{B}_i$ from $\mathbf{b}_i$. Then, the system of equations in Eq. (1) can be written in matrix-vector form by combining the bias fields $\mathbf{B}_i$ into a $mpq \times pq$ matrix $\mathbf{B}$, and combining and lexicographically ordering the images $\mathbf{g}_i$, $\mathbf{b}_i$ and $\mathbf{n}_i$ as $pq \times 1$ vectors, that is,

$$\begin{bmatrix} \mathbf{g}_1 \\ \mathbf{g}_2 \\ \cdot \\ \cdot \\ \\ \mathbf{g}_n \end{bmatrix} = \begin{bmatrix} \mathbf{B}_1 \\ \mathbf{B}_2 \\ \cdot \\ \cdot \\ \cdot \\ \mathbf{B}_n \end{bmatrix} \mathbf{f} + \begin{bmatrix} \mathbf{n}_1 \\ \mathbf{n}_2 \\ \cdot \\ \cdot \\ \\ \mathbf{n}_n \end{bmatrix},$$

which can be written in a compact form as

$$\mathbf{g} = \mathbf{B}\mathbf{f} + \mathbf{n}. \tag{2}$$

Based on the degradation model in Eq. (2), a spatially adaptive constrained least squares solution can be obtained by minimizing the following functional

$$M_w(\lambda(\mathbf{f}), \mathbf{f}) = \| \mathbf{g} - \mathbf{B}\mathbf{f} \|^2_{\mathbf{W}_1} + \lambda(\mathbf{f}) \| \mathbf{C}\mathbf{f} \|^2_{\mathbf{W}_2}, \tag{3}$$

where $\lambda(\mathbf{f})$ is the Lagrangian multiplier, $\mathbf{C}$ is a high-pass operator (e.g., discrete Laplacian), and $\mathbf{W}_1$ and $\mathbf{W}_2$ are complementary diagonal weighting matrices with $\mathbf{W}_1 = \mathbf{I} - \mathbf{W}_2$. As is well known, the parameter $\lambda(\mathbf{f})$ controls the trade-off between the fidelity to the data introduced by the term $\| \mathbf{g} - \mathbf{B}\mathbf{f} \|^2_{\mathbf{W}_1}$ and the smoothness of the solution imposed by the term $\| \mathbf{C}\mathbf{f} \|^2_{\mathbf{W}_2}$, and is therefore also called the regularization parameter. The spatial adaptivity is introduced by choosing appropriately the matrices $\mathbf{W}_1$ and $\mathbf{W}_2$ depending on the unknown image $\mathbf{f}$. We will discuss their selection in Sec. 4.

3. ITERATIVE ALGORITHM

A closed form solution of the minimizer of the functional $M_w(\lambda(\mathbf{f}), \mathbf{f})$ in Eq. (3) with respect to all unknowns $(\lambda(\mathbf{f}), \mathbf{f})$ can not be found because it is not linear. Therefore an iterative minimization procedure has to be applied, where the unknown image $\mathbf{f}$ and the regularization parameter $\lambda(\mathbf{f})$ are estimated in successive steps.

In the first step, we consider the necessary condition for a minimum of $M_w(\lambda(\mathbf{f}), \mathbf{f})$ by taking its derivative with respect to $\mathbf{f}$ and setting it equal to zero. Thus, the optimal $\mathbf{f}$ satisfies

$$\left[\mathbf{B}^H \mathbf{W}_1^T \mathbf{W}_1 \mathbf{B} + \lambda(\mathbf{f}) \mathbf{C}^T \mathbf{W}_2^T \mathbf{W}_2 \mathbf{C}\right] \mathbf{f} = \mathbf{B}^H \mathbf{W}_1^T \mathbf{W}_1 \mathbf{g}, \tag{4}$$

where $\mathbf{B}^H$ is the Hermitian transpose of $\mathbf{B}$. Due to the high dimensionality of the vector and matrices involved the direct solution of this equation is hard to obtain. Instead one can adopt numerical approaches such as gradient descent or conjugate gradient to find an estimate for the unknown image $\mathbf{f}$.

In the second step, we define the functional form of the regularization parameter $\lambda(\mathbf{f})$, so that the functional $M_w(\lambda(\mathbf{f}), \mathbf{f})$ is convex and has a unique global minimizer. This can be accomplished by satisfying three properties (see [5] for details) which result in

$$\lambda(\mathbf{f}) = f(M_w(\lambda(\mathbf{f}), \mathbf{f})) = \gamma_1 M_w(\lambda(\mathbf{f}), \mathbf{f}), \tag{5}$$

and

$$\lambda(\mathbf{f}) = \frac{\| \mathbf{g} - \mathbf{B}\mathbf{f} \|^2_{\mathbf{W}_1}}{(1/\gamma_1) - \| \mathbf{C}\mathbf{f} \|^2_{\mathbf{W}_2}}, \tag{6}$$

where γ_1 is a coefficient that controls the convexity. We choose it as $\gamma_1 = \frac{1}{2\|\mathbf{g}\|^2}$ to guarantee convergence and convexity [5, 6].

Note that all matrix operations described above can be implemented using operators, therefore the memory requirement of the proposed algorithm is small.

4. CHOICE OF THE WEIGHTING MATRICES

The weighting matrices $\mathbf{W}_1$ and $\mathbf{W}_2$ control the amount of smoothing at each pixel location depending on the strength of the intensity variation at that pixel that can be computed in a number of ways. For the pixels with high spatial activity the corresponding entries of $\mathbf{W}_2$ are very small or zero, which means that no smoothness is enforced, while for the pixels in a flat region the corresponding entries of $\mathbf{W}_2$ are very large, which means that smoothness is enforced. This matrix $\mathbf{W}_2$ has also been referred to as the visibility matrix [7] since it describes the masking property of the human visual system, according to which noise is not visible in high spatial activity regions (its high frequencies are masked by the edges), while it is visible in the low spatial frequency (flat) regions. The visibility matrix and its complementary matrix have been used in iterative image restoration in [6].

Based on our experiments, in this paper we utilize the local variance matrix $\Theta(\mathbf{f})$ given by

$$\Theta(\mathbf{f}) = \begin{bmatrix} \sigma_1^2 & 0 & 0 & \cdot & \cdot \\ 0 & \sigma_2^2 & 0 & \cdot & \cdot \\ \cdot & 0 & \sigma_3^2 & 0 & \cdot \\ & & & \cdot & \\ & & & & \sigma_{pq}^2 \end{bmatrix}, \tag{7}$$

where σ_i^2 is the local variance within a window around the pixel i. Then the weighting matrices can be calculated as follows

$$\mathbf{W}_1 = \mathbf{I} - \mathbf{W}_2 = \mathbf{I} - \frac{\Theta(\mathbf{f})}{\gamma_f}, \tag{8}$$

where γ_f is the maximum of the entries of $\Theta(\mathbf{f})$, i.e., $\gamma_f = \| \Theta(\mathbf{f}) \|_\infty$.

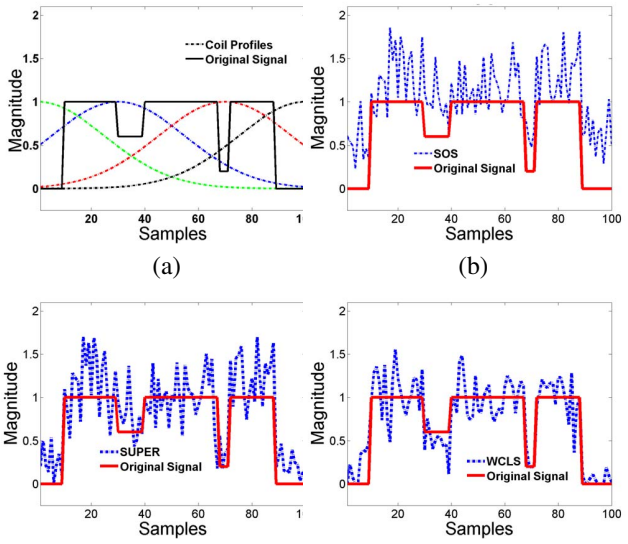

Fig. 1. Results of restoring a simulated 1D object profile. (a) Four Gaussian-shaped coil sensitivity functions (in color) and the original object profile; the recovered profiles using (b) SOS, (c) SUPER and (d) the proposed method. The original object profile is also shown in (b), (c) and (d) for comparison.

5. EXPERIMENTAL RESULTS

We performed a number of experiments using the proposed algorithm. We will present here results with both synthetic and real data to show the performance of the algorithm compared to the SOS [2], SUPER [3], and real-SUPER algorithms [3]. The real data experiments consist of phantom and in vivo studies. Phantom studies were performed using a 3.0T clinical MRI scanner (Siemens Magnetom Trio), and for the in vivo studies we used a 1.5T Siemens Magnetom Avanto. All experiments used a standard GRE sequence with the following parameters: TR/TE=100/10ms (phantom), 60/13ms (in vivo), BW = 630Hz, flip angle = 30 , and slice thickness = 5mm. 6 channels of anterior body coil were selected for imaging a Siemens Multipurpose MRI phantom. An additional image of the same slice position was acquired from the body coil for both studies.

To obtain estimates for the bias fields of the surface coils, we acquired in addition an image from the whole body coil without bias but with a high noise level. The coil sensitivities are then approximately estimated by dividing the whole body coil image by each surface coil image. In our volunteer study, the image acquisition parameters are set so that the surface coil images and the whole body coil image are acquired consecutively within a breath-hold (20 sec). Of course, these estimates are very crude, but as shown below, high quality restorations are obtained using the proposed algorithm. For all experiments, the criterion $\| \mathbf{f}^k - \mathbf{f}^{k-1} \|^2 / \| \mathbf{f}^{k-1} \|^2 < 10^{-6}$ is used to terminate the iterative procedure, and similarly the CG threshold is set to 10^{-6}. In the experiments with images, a 3x3 window is used to calculate the local variances in the proposed algorithm.

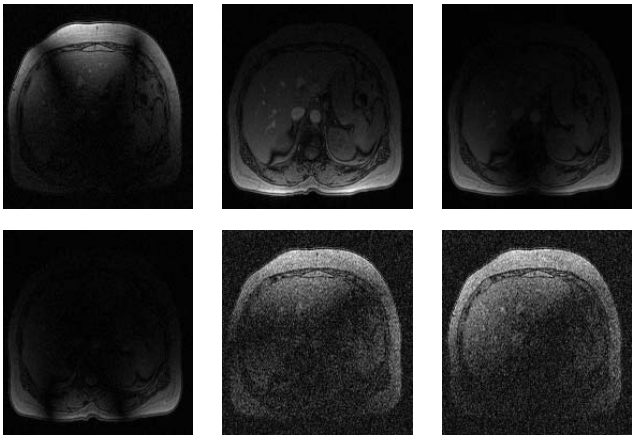

Fig. 2. Six surface coil images of the abdomen of a volunteer.

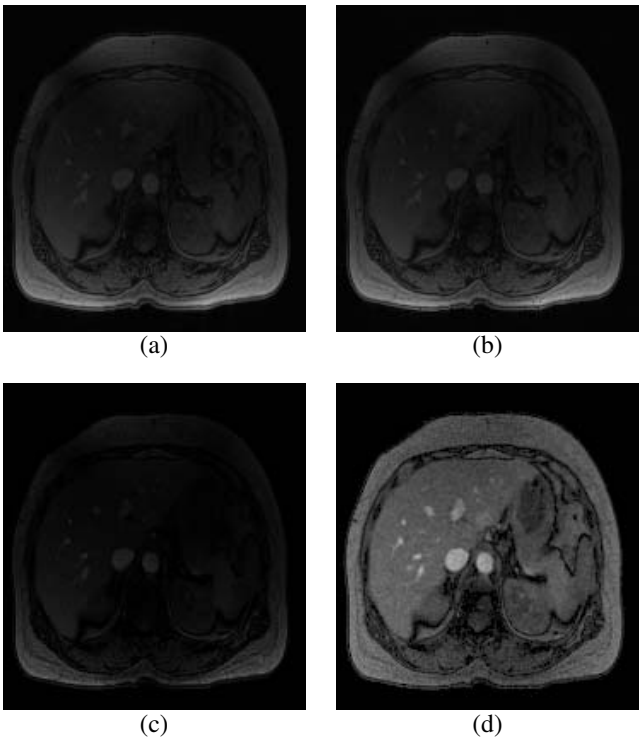

Fig. 3. Combination results of the images in Fig. (2) using the (a) conventional SOS method, (b) the SUPER method, (c) the real-SUPER method and (d) the proposed approach.

In the first experiment we simulated an 1D object multiplied by 4 Gaussian-shaped bias fields, and zero mean Gaussian noise with variance 0.1 is added so that the resulting SNR = 10dB. The original signal and the bias fields are shown in Fig. 1(a). The restored signals by the methods SOS, SUPER, and WCLS are shown in Figs. 1(b)-(d). For WCLS, a 5 pixel window is used to calculate the local variances, and Eq. (4) is

solved using successive approximation iterations. The corresponding sum of squared errors (SSE) are 20.72, 10.53, and 5.72, respectively. It is clear from the restored signals and the SSEs that the proposed algorithm outperforms the other algorithm significantly.

In the second experiment, algorithms are applied to surface coil images of a human abdomen. The acquired images are shown in Fig. (2). It is clear that some images are degraded by strong bias fields, whereas other images have a more homogeneous intensity profile but have low SNR. The combined images using the SOS, SUPER, real-SUPER, and WCLS algorithm are shown in Fig. (3). It is clear that the former methods fail to remove the bias fields completely, and the noise level is not significantly decreased. On the other hand, the bias in the combined image of WCLS is almost completely eliminated where at the same time the image is very smooth and practically noise-free.

The resolution in the combined image is of high importance in medical applications. Since the proposed algorithm incorporates smoothing in its formulation, this can present a practical problem. Therefore, to demonstrate the performance of WCLS in maintaining the high resolution, in the last experiment we apply the algorithms to surface coil images of a grid phantom. The results of the algorithms are shown in Fig. (4). Note that again, the existing methods can not completely remove the bias fields and there is a substantial level of noise but there is no loss of resolution. It is also clear that WCLS provides an image with much higher quality in terms of noise and bias removal. Additionally the high resolution is preserved which can be clearly observed from the top-left and bottom-right areas where the holes are placed very close to each other. Finally, it should be noted that the amount of smoothing can be decreased by adjusting the window size in calculating Eq. (7) or completely removed by setting $\lambda(\mathbf{f}) = 0$.

The proposed algorithm is computationally more intensive than other methods mainly because of the CG iterations required to solve Eq. (4). However, the MATLAB implementation of the algorithm required on the average under 10 seconds on a 3.20 GHz Xeon PC for 384x192 images. Therefore the running time of the algorithm is quite acceptable considering the level of the increase in the final image quality.

6. CONCLUSIONS

In this paper we represented an novel algorithm to combine MR surface coil images. We adopted a weighted constrained least squares formulation which resulted in an iterative restoration algorithm. The proposed algorithm incorporates spatial-adaptivity in the restoration process. Additionally, parameter estimation is performed at each iteration so that the algorithm works automatically without any assumptions. Experimental results demonstrate that the proposed algorithm significantly outperforms existing approaches with a small increase in computational complexity.

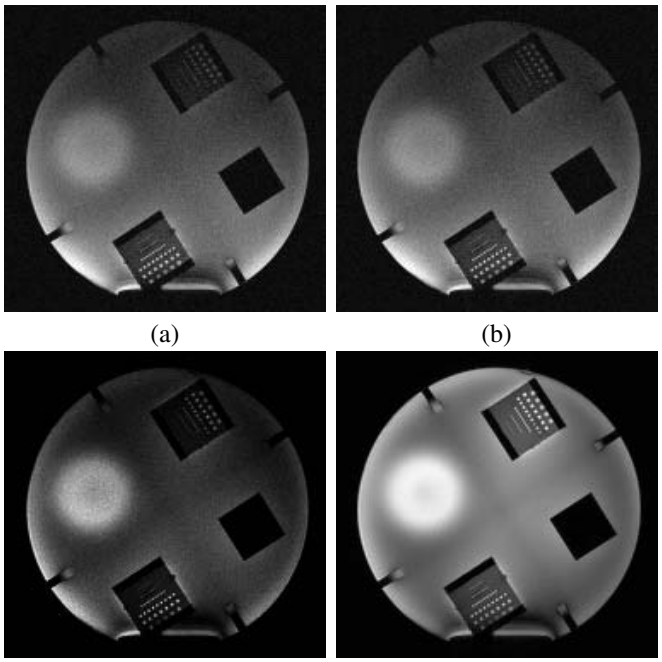

(a) (b) (c) (d)

Fig. 4. Combination results of the coil images of a grid phantom using the (a) conventional SOS method, (b) the SUPER method, (c) the real-SUPER method and (d) the proposed approach.

7. REFERENCES

[1] L. Axel, "Surface coil magnetic resonance imaging," *J Comput Assist Tomogr*, , no. 3, pp. 381–384, 1984.

[2] P. B. Roemer, W. A. Edelstein, C. E. Hayes, S. P. Souza, and O. M. Mueller, "The NMR phased array," *Magnetic Resonance in Medicine 16*, p. 192225, 1990.

[3] M. Bydder, D.J. Larkman, and J.V. Hajnal, "Combination of signals from array coils using image-based estimation of coil sensitivity profiles," *Magnetic Resonance in Medicine 47*, p. 539548, 2002.

[4] A. Fan, W. M. Wells III, J. W. Fisher III, M. Cetin, S. Haker, R. Mulkern, C. Tempany, and A. S. Willsky, "A unified variational approach to denoising and bias correction in MR," in *Proceedings of IPMI 2003*. July 2003, pp. 148–159, Springer LNCS 2732.

[5] M. G. Kang and A. K. Katsaggelos, "General choice of the regularization functional in regularized image restoration," *IEEE Trans. Image Processing*, vol. 4, pp. 594–602, 05/1995 1995.

[6] A. K. Katsaggelos and M. G. Kang, "A spatially adaptive iterative algorithm for the restoration of astronomical images," *International Journal of Imaging Systems and Technology*, vol. 6, no. 4, pp. 305–313, 1995.

[7] G. L. Anderson and A. N. Netravali, "Image restoration based on a subjective criterion," *IEEE Trans. Syst., Man, Cybern. 6*, pp. 845–853, 1976.